39th IAHR WORLD CONGRESS
GRANADA, SPAIN 2022
From Snow to Sea
19-24 June 2022

Proceedings of the 39th IAHR World Congress
19-24 June 2022
Granada, Spain
DOI number

Scour of Sand Beds by Long and Short Impinging Jets- Similarities and Differences

Mahmud Rashedul Amin[1], Nallamuthu Rajaratnam[2] and David Zhu[3]

[1,2,3] University of Alberta, Edmonton, Canada,
mamin@ualberta.ca, nrajaratnam@ualberta.ca, dzhu@ualberta.ca

Abstract

A good number of studies were conducted previously on the scour of sand beds by vertically impinging circular jets since it represents many practical scour phenomena. These studies were based on mostly long impinging jets, where the impinging height h is longer than 8.3 times the jet diameter d. However, in many practical applications, a short impinging jet with $h < 5.5d$ is desired so that the average velocity of the jet at the impingement region is higher and more uniform. This study focuses on the differences and similarities of long and short impinging jet scour, based on laboratory experiments and previous studies. Preliminary results suggest that the scour mechanism, development of scour hole, and profile of the dimensionless shape are different.

Keywords: Sand bed scour; Circular jet; Cohesionless soil; Jet impingement

1. INTRODUCTION

Scour is an important and practical problem. Failure of hydraulic structures is often associated with uncontrolled scour around the foundation. Scour in cohesionless soil is of particular interest because the bed of many natural streams is composed of cohesionless soil. Many researchers used a submerged impinging circular jet to investigate the erodibility of soils (e.g., (Doddiah et al., 1953; Poreh and Hefez, 1967; Westrich and Kobus, 1973; Aderibigbe and Rajaratnam, 1996; Ansari et al., 2003; Mazurek and Hossain, 2007; and others). However, these studies mostly used a jet with a long impinging height. Based on the observations of Rajaratnam and Beltaos (1977), a jet can be considered either a long or short jet if the impinging height h>8.3d, or h<5.5d, respectively, where d is the jet nozzle diameter. Jet impinging heights between this range (5.5d<h<8.3d) is considered as the transition region. Scour by a short impinging jet is important because it involves a stronger jet with more scouring potential. Many engineering applications involve scouring by a short jet, e.g., underwater jet trenching operation (Zhang et al., 2017), fluidization of stream beds by jets for dredging (Sullivan, 2000), and for clam harvesting (Manning, 1960). Although a few studies involved experiments with short jets (Aderibigbe and Rajaratnam, 1996; Rajaratnam and Beltaos, 1977), these studies lack adequate experimental data. Only recently, Amin et al. (2021) conducted laboratory experiments with short impinging jets and reported some interesting experimental results.

This study compares the results of short impinging jet experiments in contrast to the results of long impinging jet experiments based on previous experimental data, and some new experiments conducted in the laboratory. Flow regimes and scour mechanism for the short impinging jet are discussed based on the newly obtained experimental results. It will enhance the understanding of scour in conhesionless beds with jets of different impinging heights.

2. EXPERIMENTAL SETUP AND EXPERIMENTS

Two sets of experiments were conducted in the Belch Hydraulic lab at the University of Alberta. The first set contains a Particle Image Velocimetry (PIV) experiment of the half-model of a scour hole. A 1.5 m long, 0.5 m wide, and 0.25 m deep plexiglass sandbox was kept inside a 10 m long, 0.8 m wide, and 0.8 m deep glass-walled tank. The sand box was filled with sand of mean grain size D_{50} = 0.54 mm. A well-designed nozzle of diameter d = 12.5 mm was attached to the end of a vertical PVC pipe to create the jet. The nozzle was kept 50 mm above the sand bed so that the impinging height h of the jet was short ($h = 4d$). The tank was filled with water up to a depth of 0.6 m so that the sand bed and the jet nozzle were remained submerged during the experiment. A 0.5 hp centrifugal pump delivered water to the PVC pipe so that the jet velocity at nozzle U_j = 2.69 ms^{-1}. The PVC pipe was kept within 2-3 mm from the sidewall of the tank to create a half-model arrangement. This arrangement is also used by Pagliara et al. (2008), and others to facilitate the observation of scour dynamics from the side of the tank. The equivalent full-model jet diameter is given by $d_{full}=\sqrt{2}\,d$, while the

jet velocity for the full and half-model remains the same. The scour hole was illuminated with a led lamp from the side of the tank. A high-speed camera (Phantom v211, Vision Research, Wayne, New Jersey) was positioned at the side of the tank focusing on the center of the sand box. The camera recorded the motion of the sand particles inside the scour hole at a frequency of 1000 images per second. The PIV analysis of the sand motion was conducted using the PIVlab software (Thielicke and Stamhuis, 2014). Figure 1 shows the definition sketch of the experiments.

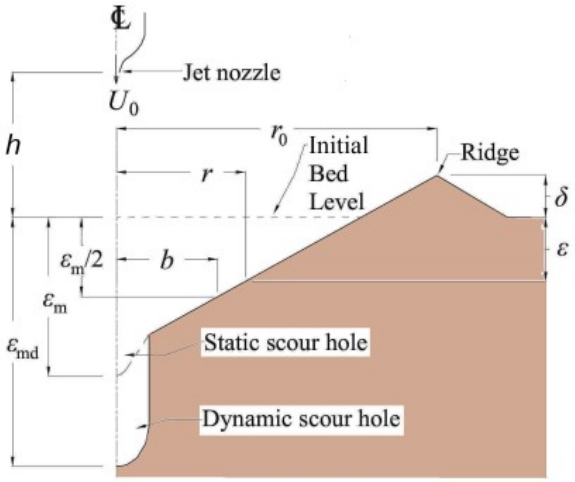

Figure 1. Definition sketch of the experiments.

The second set of experiments was conducted inside a hexagonal plexiglass tank with a full-model setup. A point gauge was used for the static dimensions of the scour hole while a depth rod was used for the dynamic depth measurement. Details of this setup can be found in Amin et al. (2021). Table 1 shows the details of the experiments.

Table 1. Summary of the experiments (partially adapted from Amin et al. 2021)

Exp. No.	D_{50} (mm)	Q (L/s)	U_j (m/s)	h (mm)	h/d	Re	Remarks
1-B-4	0.54	0.33	2.69	50	4	33614	PIV experiments
2-S-0	0.54	0.26	2.12	0	0	26483	Scour testing with
2-S-2	0.54	0.26	2.12	25	2	26483	static and
2-S-4	0.54	0.26	2.12	50	4	26483	dynamic depth
2-B-0	0.54	0.32	2.61	0	0	32595	measurements
2-B-2	0.54	0.32	2.61	25	2	32595	
2-B-4	0.54	0.32	2.61	50	4	32595	

Note: $Re=U_jd/v$ = jet Reynolds number, where v is the kinematic viscosity of water; Q = flow rate.

3. RESULTS AND DISCUSSIONS

3.1 Sand motion

Based on the flow pattern inside the scour hole, previous attempts have been made to classify the flow regimes inside the scour hole. Rouse (1940) observed the flow pattern for impingement of a vertical plane jet inside the scour hole in cohesionless soil. He termed the flow pattern as 'maximum jet deflection' when the jet deflects nearly at 180° angle and 'minimum jet deflection' when the flow follows the boundary of the scour hole up to the ridge. Similarly, Aderibigbe and Rajaratnam (1996) termed the flow pattern inside the scour hole as 'strongly deflected jet regime (SDJR)' and 'weakly deflected jet regime (WDJR)', respectively. They have identified that for $0.14 \leq E_c \leq 0.35$, the flow regime is WDJR and for $E_c > 0.35$, the flow regime is SDRJ. For short impinging jet scour, typically E_c is well above 0.35, unless either the jet velocity or jet diameter is too small. Flow pattern in SDRJ flow regime is both complex and interesting, because of the recirculatory flow and sediment-flow interaction in vortices inside the scour hole. Multiple vortices may form inside the scour hole which entrap sediments in suspended motion. When the jet is stopped, the sediments suspended in vortices settle down and thus reduce the depth of scour hole. Therefore, for SDRJ flow regime, the static and dynamic depth of scour are different. It is important to study the sediment motion inside the scour hole for a short impinging jet to understand the scour process for such jet.

Figure 2 shows the PIV results for the half-model setup. The streamlines and the vorticity map show the presence of multiple vortices. Considering only the major vortices, two vortices are present just before the opposite ridges and rotate in opposite directions. A central vortex is present beside the impinging jet, which spontaneously moves around the jet. The deflected jet carries sediment from the bottom of the scour hole and feeds sediments to these vortices. Due to the difference in sediment and water density, and centrifugal force of the vortices, bigger sand particles get more momentum that sets them free from the vortex and they move towards the ridge. Thus with time the ridge gets taller. The sediments that remain suspended in the vortices fall to the bottom of scour hole if the jet is stopped, resulting in static scour depth. The vortices near the ridge keep a dynamic equilibrium between the scour hole sidewall and the deflected jet. The sand on the sidewall slides down into the scour hole, while the deflected jet pushes them outside of the scour hole. The vortices rotate between the sidewall and the jet to keep a dynamic equilibrium.

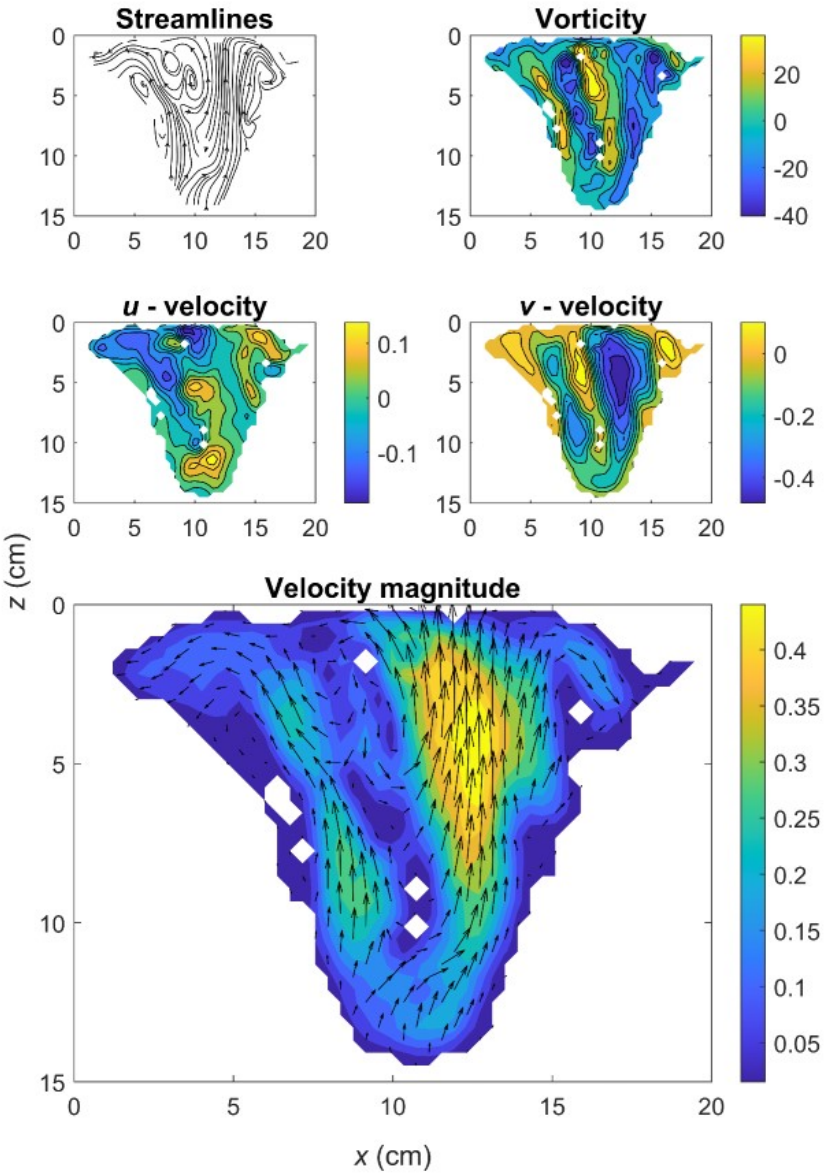

Figure 2. Sand motion inside the scour hole. Velocity and vorticity units are ms-1 and s-1, respectively.

In Figure 2, the *u* and *v* - velocity components in the positive *x* and *z* directions are positive, respectively. The *u* – velocity component shows that the sediments are accelerating towards the ridges, while the *v* – velocity component shows that the sediments are being carried to the upward direction by the deflected jet. Combined effects of the *u* and *v* – velocity components are shown in the velocity magnitude figure with velocity vectors.

3.2 Dimensions of the scour hole in steady-state

Aderibigbe and Rajaratnam (1996) showed that the length scales of the scour hole in steady-state is a function of the dimensionless quantity, the erosion parameter (E_c), given by

$$E_c = \frac{U_j\left(\frac{d}{h}\right)}{\sqrt{\left(\frac{\rho_s - \rho_w}{\rho_w}\right) g D_{50}}} \quad [1]$$

However, E_c itself is a function of the densiometric Froude number ($Fr = U_j/\sqrt{[\{(\rho_s-\rho_w)/\rho_w\}\, gD_{50}]}$, and the relative impinging height (h/d). Here, ρ_s and ρ_w are the dencity of sand and water, respectively. For the jet nozzle very close to the sand bed (i.e., $h/d \approx 0$), E_c becomes extremely big ($E_c \rightarrow \infty$). Further, Beltaos & Rajaratnam (1974) showed that for short impinging jets, the effect of d becomes significant in the flow regime compared to h. Therefore, Haehnel et al. (2006), and recently Amin et al. (2021) proposed the following modification to the erosion parameter,

$$E_c = \frac{U_j\left(\frac{d}{h+d}\right)}{\sqrt{\left(\frac{\rho_s - \rho_w}{\rho_w}\right) g D_{50}}} \quad [2]$$

The calculated E_c values in this study are based on Eq. 2. According to Aderibigbe and Rajaratnam (1996), the characteristic lengths of the scour hole in steady-state can be expressed by a power function of E_c,

$$\frac{\chi_\infty}{h+d} = C_1 {E_c}^m - C_2 \quad [3]$$

where C_1, C_2, and m are constants. χ_∞ is the characteristic length of the scour hole at steady-state. Eq. 3 is verified for long impinging scour test results obtained from the studies of Aderibigbe and Rajaratnam (1996), Ansari et al. (2003), and Rajaratnam (1982), and shown in Figure 3.

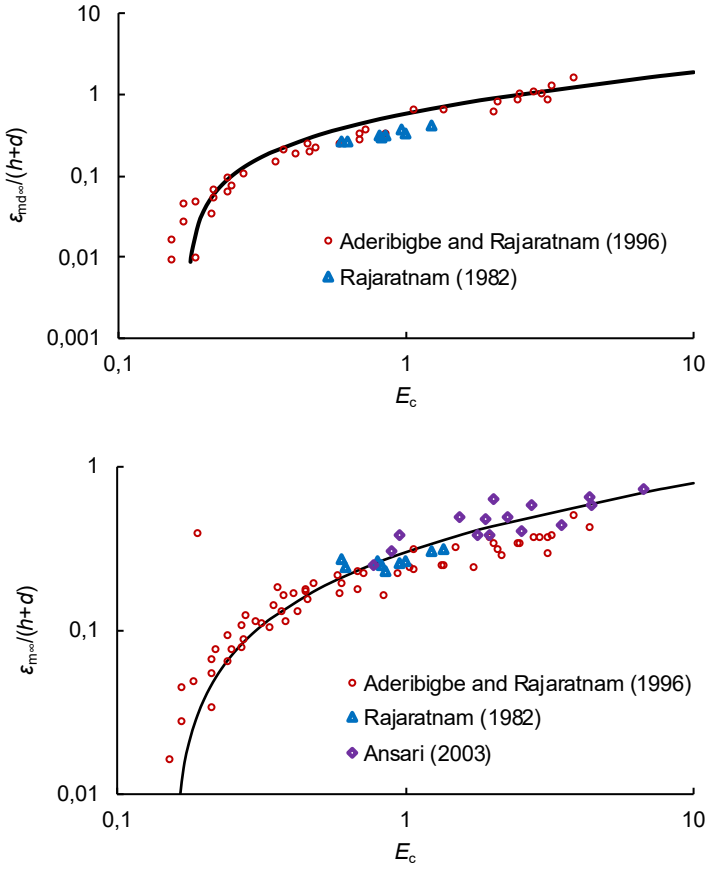

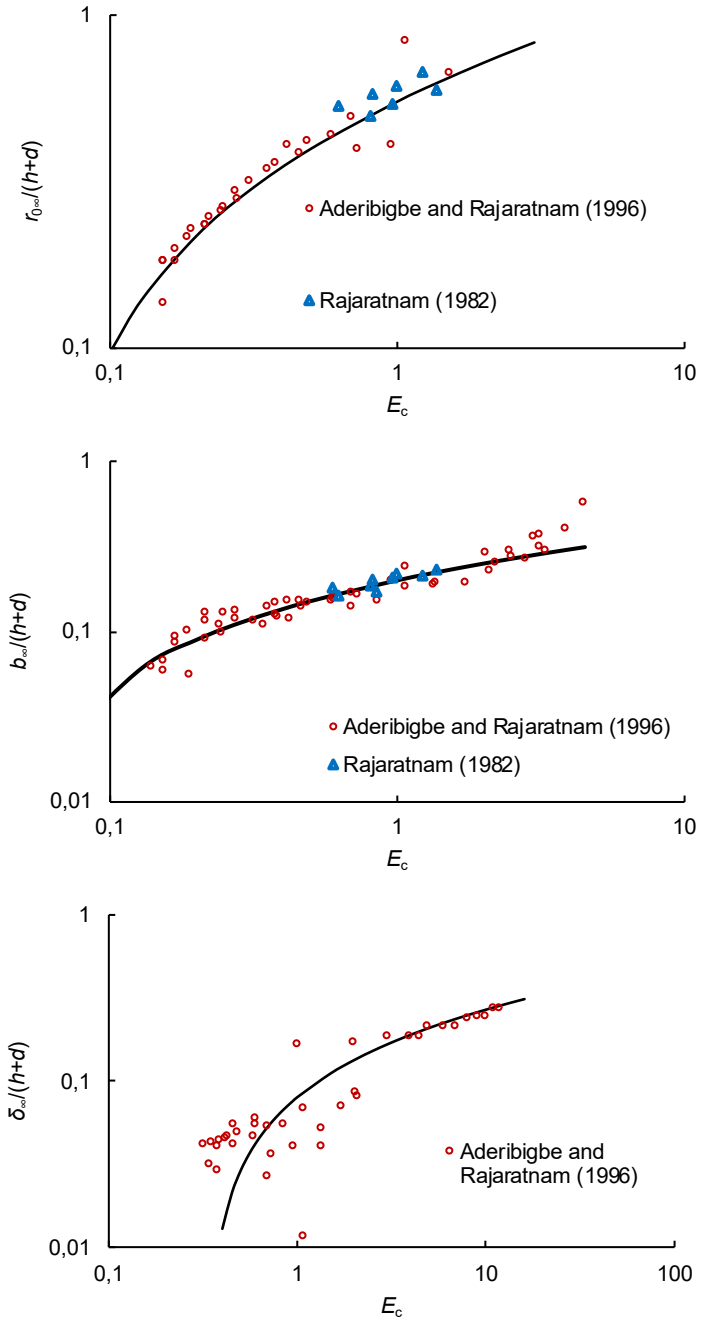

Figure 3. Characteristic lengths of the scour hole at steady state as a function of E_c for scour by long impinging jets. Note that the subscript ∞ in the figure indicate the dimensions in steady-state.

For all the cases, the power function as presented in Eq. 2 fits well the characteristic lengths with R^2 between 0.80 and 0.91. However, for short impinging jet scour, the scour test data reported in Amin et al. (2021) shows that a linear function of Ec can be used to predict the characteristics scour dimensions,

$$\frac{\chi_\infty}{h+d} = C_3 E_c - C_4 \qquad [4]$$

where C_3 and C_4 are constants. Figure 4 shows the characteristic dimensions of the scour hole at steady-state for scour by short impinging jet. Eq. 4 fits the characteristic dimensions well with R^2 between 0.90 to 0.98. Amin et al. (2021) attributed the difference in the functional relations between the characteristic dimensions and E_c on the sediment and jet inter-action in different flow regimes for long and short impinging jets.

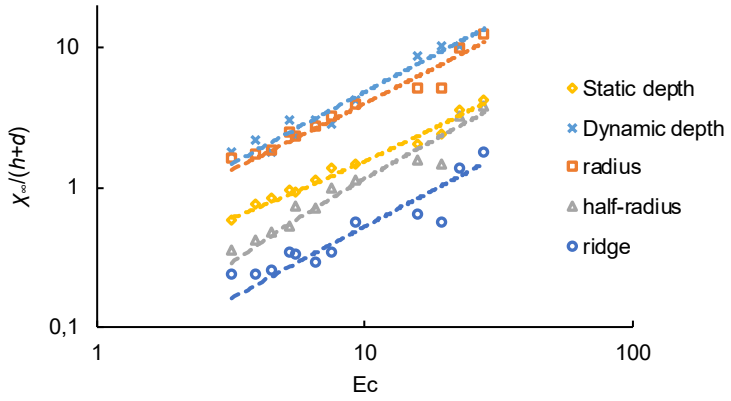

Figure 4. Characteristic lengths of the scour hole at steady state as a function of Ec for scour by short impinging jets

3.3 Similarity of profiles at steady state

Similar to the observation of the long impinging jet experiments, dimensionless profiles of the scour hole at steady-state also show self-similarity for short impinging jets. Figure 5a shows scour hole profiles for scour tests with with U_j = 2.12-2.61 ms^{-1}, h = 0 – 50 mm, d = 12.5 mm, and D_{50} = 0.54 mm. Figure 5b shows that the dimensionless profiles for all the tests collapse into a single profile. For long impinging jet experiments, the dimensionless profile is Gaussian (Aderibigbe and Rajaratnam, 1996). However, for short impinging jets, this profile has linear side slope, corresponding to the submerged angle of repose of the sand (Amin et al., 2021).

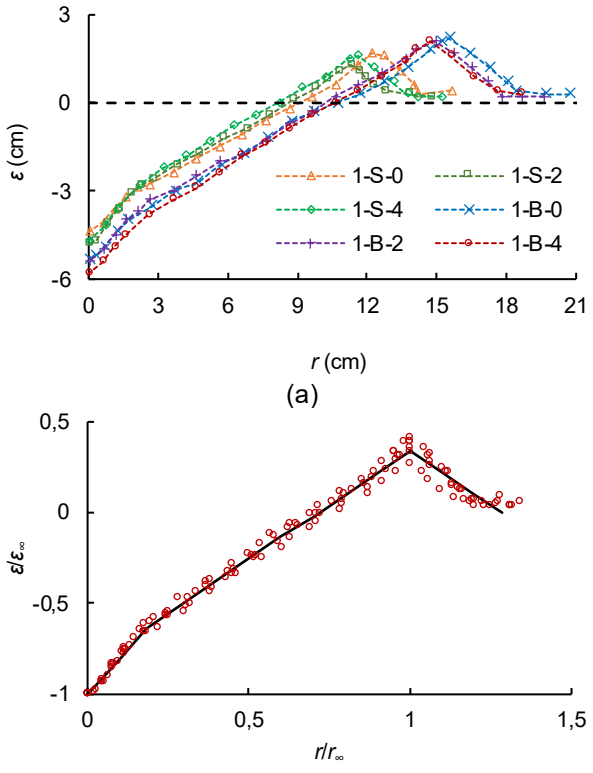

Figure 5. Scour hole profiles at steady state for (a) scour tests with U_j = 2.12-2.61 ms^{-1}, h = 0 – 50 mm, d = 12.5 mm, D_{50} = 0.54 mm; and (b) similarity in dimensionless profiles.

4. CONCLUSIONS

Based on previous studies on the scour of sand beds by long impinging jets, and some recent experiments with short impinging jets, this work shows a comparative study of the results of the scour experiments with jets of different impinging heights. It is found that there are some interesting and noteworthy differences in the scour

testing results for long and short impinging jets. The characteristic scour lengths for long and short impinging jets have different functional relations with the erosion parameter. The steady-state scour profiles for long and short jet experiments are also different. Particle image velocimetry (PIV) experiments were carried out to explore the sediment dynamics for short impinging jets. Experimental results showed that the short impinging jet scouring has a resemblance to the 'strongly deflected jet regime' of long impinging jets. This is because the erosion parameter for a short impinging jet experiment is typically more than 0.35, unless the jet diameter or nozzle velocity is too small.

5. ACKNOWLEDGEMENTS

The authors are thankful to Perry Fedun, the Water Resources Group Lab Supervisor for his invaluable support in the experimental setup.

.

6. REFERENCES

Aderibigbe, O., and Rajaratnam, N. (1996). Erosion of loose beds by submerged circular impinging vertical turbulent jets. *Journal of Hydraulic Research*, 34(1), 19–33.

Amin, M.R., Rajaratnam, N., and Zhu, D.Z. (2021). Scouring of sand beds by short impinging turbulent jets. *Proceedings of the Institution of Civil Engineers - Water Management*, 174(6), 309–320.

Ansari, S.A., Kothyari, U.C., and Raju, K.G.R. (2003). Influence of Cohesion on Scour under Submerged Circular Vertical Jets. *Journal of Hydraulic Engineering*, 129(12), 1014–1019.

Beltaos, S., and Rajaratnam, N. (1974). Impinging circular turbulent jets. *Journal of the Hydraulics Division*, 100(10), 1313–1328.

Doddiah, D., Albertson, M.L., and Thomas, R. (1953). Scour from Jets. In *Proceedings of 5th IAHR Congress, International Association for Hydraulic Research, Minneapolis, CO, USA*. International Association for Hydraulic Research, Madrid, Spain, pp. 161–169.

Haehnel, R.B., Cushman-roisin, B., and Dade, W.B. (2006). Cratering by a subsonic jet impinging on a bed of loose particles. In *Proceedings of Earth and Space 2006 - 10th Biennial International Conference on Engineering, Construction, and Operations in Challenging Environments*, Houston, TX, United states, pp. 1-8.

Manning JH (1960) Commercial and biological uses of Maryland clam dredge. In *Proceedings of the 12th Annual Gulf and Caribbean Fisheries Institute*. Gulf and Caribbean Fisheries Institute, Coral Gables, FL, USA, pp. 61–67.

Mazurek, K.A., and Hossain, T. (2007). Scour by jets in cohesionless and cohesive soils. *Canadian Journal of Civil Engineering*, 34(6), 744–751.

Pagliara, S., Amidei, M., and Hager, W.H. (2008). Hydraulics of 3D Plunge Pool Scour, *Journal of Hydraulic Engineering*, 134 (9), 1275–1284.

Poreh M and Hefez E (1967) Initial scour and sediment motion due to an impinging jet. *Proceedings of the 12th Congress of the International Association for Hydraulic Research (IAHR), Fort Collins, CO, USA*. International Association for Hydraulic Research, Madrid, Spain, p. 8.

Rajaratnam, N. (1982). Erosion by submerged circular jets. *Journal of the Hydraulics Division*, 108(2), 262–267.

Rajaratnam, N., and Beltaos, S. (1977). Erosion by impinging circular turbulent jets. *J Hydraul Div*, 103(10), 1191–1205.

Rouse H (1939) Criteria for similarity in the transportation of sediment. In *Proceedings of 1st Hydraulic Conference*. University of Iowa, Iowa City, IA, USA, pp. 33–49.

Sullivan, N. (2000). The use of agitation dredging, water injection dredging and sidecasting: Results of a survey of ports in England and Wales. *Terra Aqua*, 78, 11–20.

Thielicke, W., and Stamhuis, E.J. (2014). PIVlab – Towards user-friendly, affordable and accurate digital particle image velocimetry in MATLAB. *Journal of Open Research Software*, 2(1), 1-10.

Westrich B and Kobus H (1973) Erosion of a uniform sand bed by continuous and pulsating jets. *Proceedings of the 15th International Association for Hydraulic Research (IAHR) Congress*, Istanbul, Turkey, pp. 91–98.

Zhang S, Ge T, Zhao M and Wang C (2017) The prediction of traveling jet trenching in stiff clay based on the erosion failure mechanism. *Marine Georesources and Geotechnology*, 35(7): 939–945.